Neoplasia • Vol. 5, No. 3, May/June 2003, pp. 187–192 187

www.neoplasia.com

Optical Imaging of Apoptosis as a Biomarker of Tumor Response to Chemotherapy[1]

Eyk A. Schellenberger[2], Alexei Bogdanov Jr., Alexander Petrovsky, Vasilis Ntziachristos, Ralph Weissleder and Lee Josephson

Center for Molecular Imaging Research, Massachusetts General Hospital, Charlestown, MA 02129, USA and Harvard Medical School, Boston, MA, USA

Abstract

A rapid and accurate assessment of the antitumor efficacy of new therapeutic drugs could speed up drug discovery and improve clinical decision making. Based on the hypothesis that most effective antitumor agents induce apoptosis, we developed a near-infrared fluorescent (NIRF) annexin V to be used for optical sensing of tumor environments. To demonstrate probe specificity, we developed both an active (i.e., apoptosis-recognizing) and an inactive form of annexin V with very similar properties (to account for nonspecific tumor accumulation), and tested the agents in nude mice each bearing a cyclophosphamide (CPA) chemosensitive (LLC) and a chemoresistant LLC (CR-LLC). After injection with active annexin V, the tumor–annexin V ratio (TAR; tumor NIRF/background NIRF) for untreated mice was 1.22 ± 0.34 for LLC and 1.43 ± 0.53 for CR-LLC ($n = 4$). The LLC of CPA-treated mice had significant elevations of TAR (2.56 ± 0.29, $P = .001$, $n = 4$), but only a moderate increase was obtained for the CR-LLC (TAR = 1.89 ± 0.19, $P = .183$). The *in vivo* measurements correlated well with terminal deoxyribosyl transferase-mediated dUTP nick end labeling indexes. When inactive Cy–annexin V was used, with or without CPA treatment and in both CCL and CR-CCL tumors, tumor NIRF values ranged from 0.91 to 1.17 (i.e., tumor were equal to background). We conclude that active Cy–annexin V and surface reflectance fluorescence imaging provide a nonradioactive, semiquantitative method of determining chemosensitivity in LLC xenografts. The method maybe used to image pharmacologic responses in other animal models and, potentially, may permit the clinical imaging of apoptosis with noninvasive or minimally invasive instrumentation.

Neoplasia (2003) **5,** 187–192

Keywords: annexin V; optical imaging; apoptosis; tumor; chemotherapy.

Introduction

A noninvasive method of predicting tumor response early in the course of a chemotherapeutic regime might find considerable use in animal models assessing drug potency, or in the treatment of human disease. Imaging extracellular-facing phosphatidylserine (PS), an early marker of apoptosis, with a technetium-labeled annexin V (Tc annexin V) has been suggested as a method of monitoring tumor response to chemotherapy [8]. As cells proceed along the pathway(s) to apoptosis, PS, a lipid normally facing the cytoplasm, flips and faces the extracellular fluid [15]. The protein annexin V binds PS strongly, specifically in a calcium-dependent fashion, which is a reflection of its biologic role as an anticoagulant [5,9,11,21,26]. PS is attractive as a target for imaging the response to chemotherapy because different forms of chemotherapy have a common propensity to induce apoptosis [7,12,14,16,24], and PS is a feature of apoptotic cells regardless of how apoptosis is induced [26]. Moreover, resistance to chemotherapy may reflect cellular mechanisms that prevent the chemotherapy from inducing apoptosis.

An optical method for imaging apoptosis would not only eliminate patient exposure to radiation and the need for frequent radiotracer synthesis—it might enable the visualization of apoptosis in settings quite different from that required of scintigraphic imaging. These might include intraoperative visualization, using surface-weighted surface reflectance imaging equipment [13,28] or, in a minimally invasive fashion, use of fluorescent endoscopes [30,31]. We therefore decided to investigate whether a near-infrared fluorescent (NIRF) form of annexin V could be developed and used in conjunction with a surface reflectance fluorescence imaging, to provide a semiquantitative method of imaging PS exposure in an animal model. Surface reflectance fluorescence imaging illuminates the animal with light that excites a fluorochrome, and acquires an image at a second longer wavelength of emitted light from the animal. We describe the synthesis of an NIRF conjugate of annexin V and

Abbreviations: NIRF, near-infrared fluorescence; CPA, cyclophosphamide; LLC, Lewis lung carcinoma; CR-LLC, chemoresistant Lewis lung carcinoma; PS, phosphatidylserine; TUNEL, terminal deoxyribosyl transferase-mediated dUTP nick end labeling

Address all correspondence to: Lee Josephson, PhD, Center for Molecular Imaging Research, Massachusetts General Hospital, Building 149, 13th Street, 5403, Charlestown, MA 02129, USA. E-mail: ljosephson@partners.org

[1]This work was supported by NIH grants RO1CA86782, P50CA86355, R24 CA92782, and CA91807.

[2]E.A.S. received a grant from the ''Deutsche Akademie der Naturforscher und Mediziner Lepoldina.''

Received 2 October 2002; Accepted 12 November 2002.

its use in imaging PS when a chemosensitive Lewis lung carcinoma (LLC) and a chemoresistant LLC (CR-LLC) were treated with cyclophosphamide (CPA). The NIRF conjugate of annexin V and our imaging technique provided a semiquantitative method of determining tumor PS that was reflected with CPA treatment and tumor chemosensitivity.

Materials and Methods

Labeling of Annexin V with Fluorescent Dyes

Annexin V was obtained from Theseus Imaging, Cambridge, MA and was identical to that used clinically. Annexin V migrated as a single band of 36 kDa by SDS-PAGE, confirming its purity (data not shown). To synthesize a Cy5.5-labeled annexin V, we added 333 μl of annexin V (3.0 mg/ml dialyzed against 0.1 M bicarbonate pH, 8.0) to a vial of the Cy5.5 *N*-hydroxysuccinimide ester (Amersham-Pharmacia, Piscataway, NJ). After 20 minutes at room temperature, the mixture was transferred into a second Cy5.5 vial and incubated for another 40 minutes at room temperature. Protein was separated from unreacted dye by two successive spin separations using 10 ml of BioGel P6 columns in PBS, pH 7.4 (Bio-Rad, Hercules, CA). The concentration of coupled Cy5.5 dye was determined spectrophotometrically ($E_{678} = 250{,}000\ M^{-1}\ cm^{-1}$). Protein was determined by the BCA method (Bio-Rad, Richmond, CA). The conjugate had 1.1 Cy5.5 attached per mole of annexin V. To synthesize annexin V–Cy5.5 conjugates with a range of dye-to-protein ratios, a vial of Cy5.5 was solubilized with 7 μl of DMSO and 1.0, 2.0, or 4.0 μl added to 30 μg of annexin V (0.1 M Na–carbonate buffer, pH 8.0) to give a final volume of 20 μl. The reaction tubes were incubated for 1.5 hours at room temperature. After adding 30 μl of PBS, pH 7.4, the protein was separated from unreacted dye by two successive spin separations using 1 ml of Biospin P6 columns equilibrated with PBS, pH 7.4 (Bio-Rad). The resulting conjugates had 1.6, 2.0, and 2.4 mol of dye molecules per mole of protein. Conjugates are referred to as $Cy5.5_n$–annexin V, where *n* is the mole of dye per mole of protein.

To synthesize a fluorescein-labeled annexin V (FITC–annexin V), 1 mg of annexin V in 200 μl of the buffer above was reacted with 200 μg of fluorescein isothiocyanate (FITC) in 1 ml of buffer for 1.5 hours at room temperature. The protein was separated from unreacted dye by dual-spin separation, as above. The concentration of coupled fluorescein was determined spectrophotometrically ($E_{494} = 72000\ M^{-1}\ cm^{-1}$). The conjugate had a ratio of 1.6 dye molecules/protein. The activity of this FITC–annexin V was similar to that from a commercial source (Clontech, Palo Alto, CA).

Cell Binding of Fluorescent Annexin V Conjugates

Jurkat T cell cells (Clone E6-1, no. TIB-152; ATCC, Manassas, VA) were grown in RPMI 1640 medium with 10% fetal bovine serum (Vitacell no. 30-2021; ATCC), which was changed every 2 or 3 days. Apoptosis was induced by the addition of 7 μl of camptothecin (1 mM in DMSO) per milliliter of culture medium and incubation for 5 to 6 hours at 37°C. Induction of apoptosis was verified by staining with propidium iodide and FITC–annexin V using a calcium-containing binding buffer (1.8 mM $CaCl_2$, 10 mM HEPES, 150 mM NaCl, 5 mM KCl, 1 mM $MgCl_2$, pH 7.4). The cells were analyzed with a FACS-Calibur cytometer (Becton Dickinson, San Jose, CA) according to the manufacturer's manual. Cells were incubated with dye–annexin V conjugates (0.1 μg of each dye–annexin V in 200 μl of binding buffer) for 10 minutes at room temperature. For competition assays, cells were incubated with a 10-fold protein excess (1.0 μg of inhibitor dye–annexin V or annexin V) for 5 minutes before the addition of dye–annexin V as above. Flow cytometry was as above.

Fluorescence Microscopy

Ten microliters of cell suspension was applied to a microscopy slide, placed on an Axiovert Ziess microscope (Carl Zeiss MicroImaging, Thornwood, NJ), and photographed by employing a SenSys CCD camera (Roper Scientific, Trenton, NJ) attached to a G4-PowerMac (Apple Computer, Cupertino, CA).

Tumor Model

LLC cell lines sensitive to and resistant to CPA were provided by Dr. Timothy Browder (Children's Hospital, Boston, MA) and have been described [3]. CPA-sensitive and CPA-resistant cell lines are denoted as CLL and CR-CLL, respectively. Cells were grown as monolayers in DMEM (Cellgro; Mediatech, Washington, DC), containing 10% inactivated FBS, 1% penicillin/streptomycin, and 0.15% L-glutamine at 37°C in a humidified 5% CO_2 atmosphere. One million cells (0.05 ml) were subcutaneously injected in female athymic nu/nu mice (28 g; Jackson Laboratory, Bar Harbor, ME). Ten and 12 days after tumor injection, the animals received CPA 170 mg/kg, i.p. (Mead Johnson, Princeton, NJ). One day after the second CPA treatment, the animals received 61 nmol/kg Cy5.5 dye, present as either active or inactive Cy–annexin V, by tail vein injection and were imaged 90 minutes later. All procedures were approved by the MGH Animal Care and Use Committee.

Optical Imaging

The animals were anesthesized with ketamine/xylazine (200/30 mg/kg, i.p). NIRF and white light images were acquired using a reflectance fluorescence imaging system as described [13,28]. To obtain tumor NIRF signals from tumors, the mean signal intensity was measured with ImageJ (National Institute of Health, USA) from hand-drawn regions of interest for each tumor or region adjacent to the tumor. The tumor mean NIRF signal was then divided by the background mean NIRF signal to obtain the tumor–annexin V ratio (TAR). The tumor margins were evident from the images of the animals, physical examination, and dissection.

Histology

After imaging, the animal was euthanized (pentobarbital, 200 mg/kg, i.p.), and tumors were excised, snap frozen, and cut into sections. Frozen sections were stained for apoptosis by a commercially available terminal deoxyribosyl

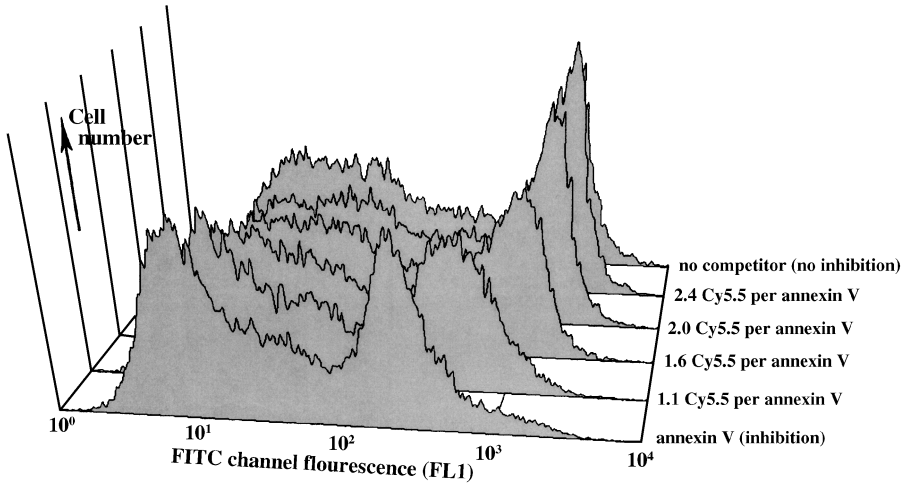

Figure 1. *Competition assay for the ability of Cy5.5–annexin V conjugates to bind PS on the surface of camptothecin-treated Jurkat T cells. Displacement of FITC–annexin V (FACS FL1 channel) with a 10-fold excess of Cy5.5–annexin V preparations labeled with increasing numbers of Cy5.5 dyes per mole of protein. As n decreases (back to front), Cy5.5–annexin Vs become more effective inhibitors of FITC–annexin V binding.*

transferase-mediated dUTP nick end labeling (TUNEL) method (ApopTag kit; Intergen, Purchase, NY). Slides were photographed using an Axiovert Ziess microscope (Carl Zeiss MicroImaging).

Results

To examine the ability of annexin V to retain its activity after modification with the dye Cy5.5, we prepared four Cy5.5–annexin Vs with different numbers of Cy5.5 attached per mole of protein. We then analyzed the conjugates in a competition assay using FITC–annexin V binding to PS on camptothecin-treated Jurkat T cells. The induction of PS exposure following treatment with camptothecin has been well studied [23,25]. Cells were incubated with the conjugate FITC–annexin V and a 10-fold excess of various Cy5.5-labeled annexin Vs or unlabeled annexin V, and cell-associated FITC fluorescence (FL1 channel) was obtained (Figure 1). Values were normalized to the median fluorescence with no added annexin V. The conjugate $Cy5.5_{-2.4}$–annexin V gave a displacement of 0.98 compared to a reference value of 1.0 for no added annexin V, and is referred to as inactive Cy–annexin V. As the number of attached Cy5.5 molecules decreased, the ability of the Cy5.5–annexin Vs to displace FITC–annexin V increased. The conjugate $Cy5.5_{-1.1}$–annexin V gave a displacement of 0.32, compared to a value of 0.17 for unlabeled annexin V. The $Cy5.5_{-1.1}$–annexin V conjugate is referred to as "active Cy–annexin V" below. Inactive Cy–annexin V serves as control material for imaging studies, with the same fluorochrome and nearly the same size as active Cy–annexin V, but unable to bind PS.

The ability of active Cy–annexin V to bind cells was further evaluated as shown in Figure 2. We incubated a mixture of active Cy5.5–annexin V and FITC–annexin V with untreated (Figure 2*A*) and camptothecin-treated cells (Figure 2*B*) and submitted them to FACS analysis. Untreated cells failed to bind either probe (91.8%) or bound both probes (7.2%; Figure 2*A*). Treated cells bound both probes (59.1%) or failed to bind either probe (36.7%; Figure 2*B*). By FACS analysis, active Cy5.5–annexin V and FITC–annexin V bound the same cells after treatment with camptothecin.

Fluorescence micrographs of cells treated with camptothecin for 7.5 hours and then stained with active Cy–annexin V, and a probe for active caspases (FITC-VAD-FMK) are shown in Figure 2*C*. As expected, active Cy–annexin V was membrane-bound (red), whereas FITC-VAD-FMK (green) gave an intense cytoplasmic stain. These doubly stained cells comprised 41.0% of cells by FACS analysis. Also shown are examples of cells that were stained for either active caspase or with active Cy–annexin V. $Caspase^{-}$/annexin V^{+} cells (14.1% of total) may represent cells that have completed camptothecin-induced apoptosis before others, because less than 5% of cells were in this state before the addition of camptothecin. Rare $caspase^{+}$/annexin V^{-} cells (4.9%) were also found.

To examine whether active Cy–annexin V might serve as an NIRF imaging agent, we imaged a mouse with chemosensitive LLCs and chemoresistant CR-LLCs implanted in the mammary fat pads after CPA treatment (Figure 3, *A*–*C*). In preliminary experiments, it was shown that tumor NIRF reached a stable peak between 75 and 1200 minutes after injection of active Cy–annexin V. An imaging time of 90 minutes postinjection was therefore chosen as optimal. Supporting this time for optical imaging are pharmacokinetic studies with Tc annexin V, which indicate that it has a blood half-life of less than 30 minutes [29]. Figure 3 shows the white light image (*A*), the raw NIRF image (*B*), and a colored NIRF image (*C*) of the mouse. The chemosensitive LLC tumor had a visibly higher signal intensity than the chemoresistant CR-LLC tumor, a result that was confirmed with region of interest (ROI) measurements of tumor signal intensity and with additional animals (see Figure 4). Also shown is a mouse implanted with chemosensitive LLC and chemoresistant CR-LLC tumors, treated with CPA and injected with inactive Cy–annexin V (Figure 3*D*). In this case, tumor NIRF was lower and only equal to background, a result again confirmed with additional animals (see below). We conclude that the

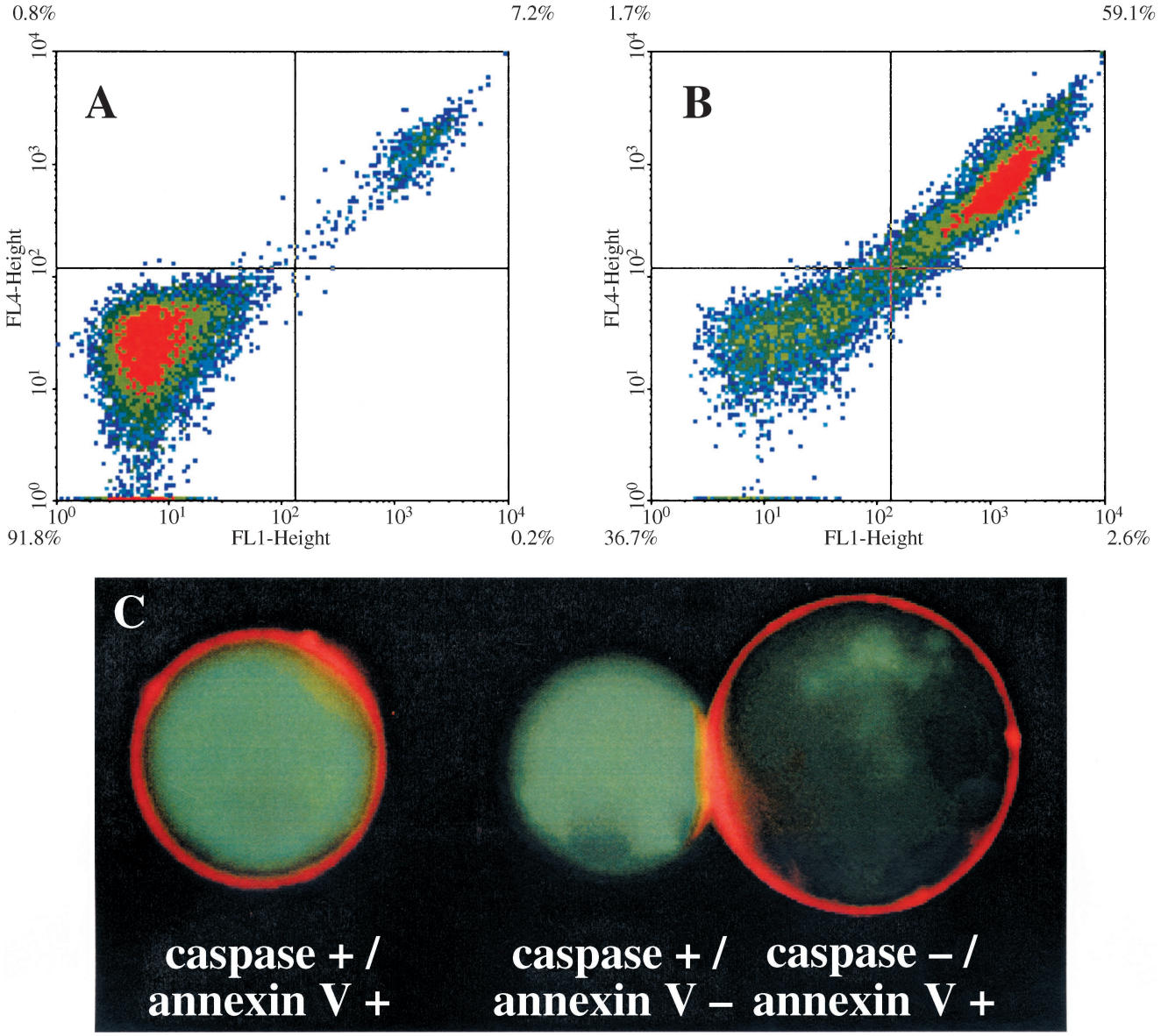

Figure 2. *Labeling of untreated and camptothecin-treated Jurkat T cells with active Cy5.5–annexin V. (A) Untreated cells incubated with active Cy–annexin V and FITC–annexin V. The FL1 channel is for fluorescein whereas FL4 is for Cy5.5. Unlabeled cells are in the left quadrant (91.8%), whereas cells labeled with both annexin Vs are in the upper right quadrant (7.2%). (B) Camptothecin-treated cells incubated with active Cy–annexin V and FITC–annexin V. Double-labeled cells are in the upper right quadrant (59.1%), with unlabeled cells in the lower left quadrant (36.7%). (C) Fluorescence micrographs of camptothecin-treated cells stained with active Cy–annexin V and the caspase probe FITC-VAD-FMK. A membrane-bound NIRF signal from active Cy–annexin V and a cytoplasmic green fluorescence from FITC-VAD-FMK are seen.*

tumor NIRF signal obtained with active Cy–annexin V depended on PS binding, rather than on some nonspecific mechanism of accumulation, based on the lack of signal obtained with inactive Cy–annexin V.

A TUNEL stain for the apoptotic cells present in LLC and CR-LLC tumors is shown in Figure 3, *E* and *F*. Using additional sections, we determined that the apoptotic index after CPA treatment was 89.1 ± 9.3 and 36.7 ± 5.1 for the LLC and CR-LLC tumors, respectively. Hence, the apoptotic index was dependent on the chemosensitivity of the tumor.

NIRF signal intensity data were quantified by taking ROI signal intensity measurements for chemosensitive LLC and chemoresistant CR-LLC tumors and for areas adjacent to the tumor, after an injection of active Cy–annexin V. Results are summarized in Figure 4. After treatment with CPA, the chemosensitive LLC had a TAR of 2.56 ± 0.29 compared to 1.89 ± 0.19 for CR-LLC, which were different at a significance of $P = .002$ using a paired Student's *t*-test. Hence, after CPA treatment, TAR was a function of tumor chemosensitivity. Also of note is the fact that CPA treatment significantly increased the TAR of both the LLC and CR-LLC tumors, and statistical significance of this increase was higher for the LLC than the CR-LLC tumor. CPA treatment increased the TAR of the chemosensitive LLC tumor (1.22 ± 0.34 to 2.56 ± 0.29, $P = .001$, unpaired Student's *t*-test), whereas the chemoresistant CR-LLC tumors had a more modest TAR increase (1.43 ± 0.53 to 1.89 ± 0.19, $P = .183$, unpaired Student's *t*-test). When inactive Cy–annexin V was injected

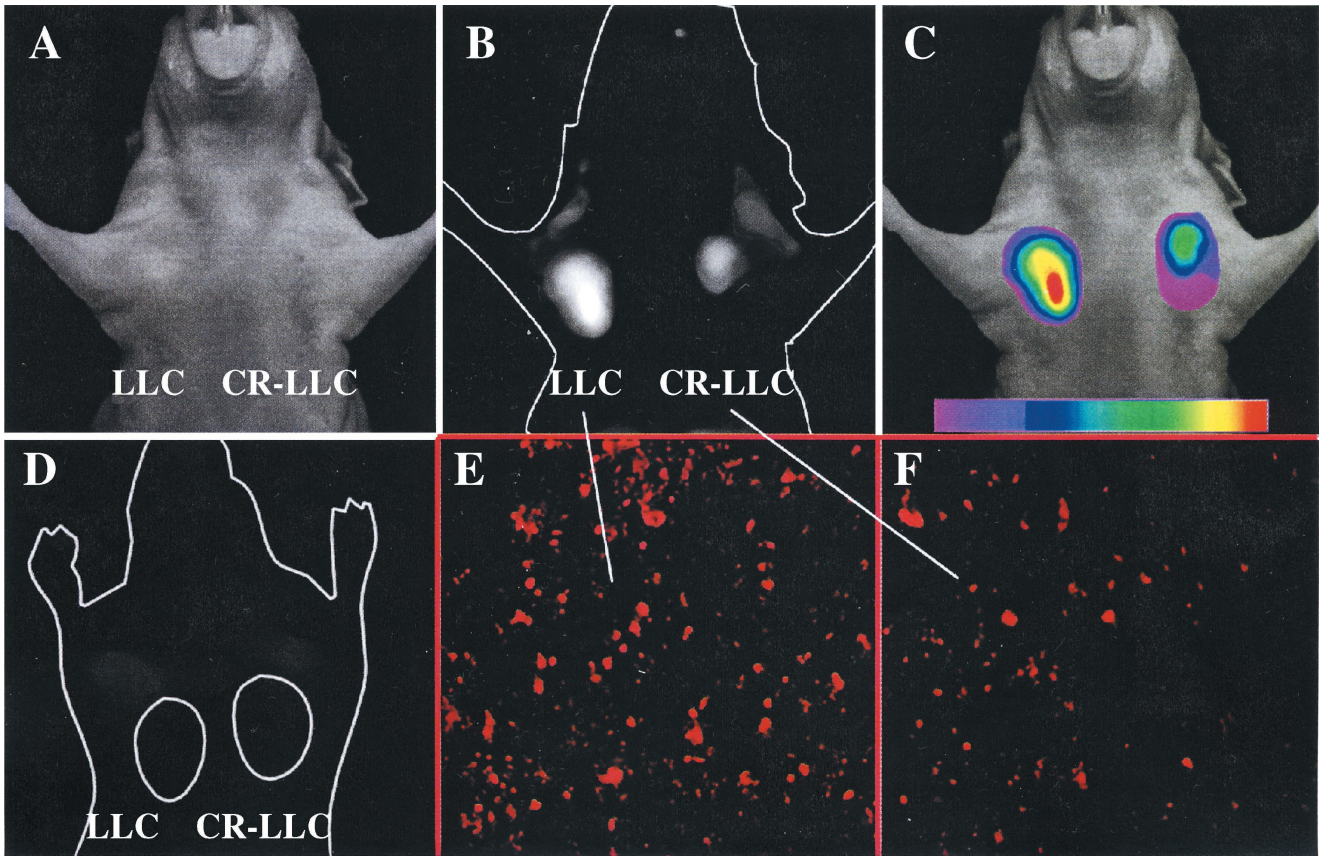

Figure 3. *In vivo imaging of LLC implanted in the mammary fat pads of nude mice. LLC indicates CPA-sensitive and CR-LLC indicates CPA-resistant tumor. (A) White light image 90 minutes after injection of active annexin V. (B) Raw NIRF image of (A). (C) Color-coded map of NIRF intensity superimposed on the white light image. (D) Raw image of tumors after CPA treatment and injection of inactive Cy annexin V. (E) TUNEL stain of the LLC tumor. (F) TUNEL stain of the CR-LLC tumor.*

into LLC and CR-LLC tumor-bearing animals, with or without CPA treatment, tumor NIRF/background NIRF values ranged from 0.99 to 1.17 and the magnitude of nontumor signal intensity (background) was similar using active Cy–annexin V or inactive Cy–annexin V.

Discussion

Active Cy–annexin V binds to LLC xenografts after treatment with CPA, yielding an NIRF signal that can be quantified from outside a nude mouse using a surface reflectance type of instrumentation. The magnitude of tumor NIRF depended on the history of CPA treatment and the sensitivity of the tumor to CPA. The tumor NIRF obtained resulted from the binding of active Cy–annexin V to PS, a conclusion based on the lack of signal obtained with inactive Cy–annexin V. Synthesis of an active and an inactive Cy–annexin V was accomplished by altering the extent of modification of the protein with the *N*-hydroxysuccinimide ester of Cy5.5 (active Cy–annexin V, 1.1 Cy5.5 dyes/annexin V versus inactive Cy–annexin V, 2.4 dyes/annexin V). Active and inactive forms of Cy–annexin V have identical amino acid sequences and compositions, and similar molecular weights. The molecular masses of annexin V and Cy5.5 are 36 and 0.900 kDa, respectively, so active Cy–annexin V [total mass = 1.1(0.900) + 36 kDa] and inactive Cy–annexin V [total mass = 2.4(0.90) + 36 kDa] differ by only 1.35 kDa. Because of the many similarities between the two forms of annexin V, inactive Cy–annexin V is an ideal probe for demonstrating that the tumor NIRF obtained with active Cy–annexin V depends on PS binding.

The accumulation of radioactive annexin V in tissues, as determined by imaging, has often been related to the extent of tissue apoptosis [1,2]. The TAR for the CPA-treated chemosensitive LLC tumor (2.56 ± 0.29) was associated with an apoptotic index of 89 ± 9.1, whereas the TAR for the chemoresistant CR-LLC tumor (1.89 ± 0.19) was associated with a lower apoptotic index of 36.7 ± 5.1. However, the value of active Cy–annexin V for imaging the effectiveness of a chemotherapeutic regime may not depend on whether the NIRF signal obtained originates only from its binding exclusively to apoptotic cells. First, PS exposure and annexin V binding are characteristics of necrotic as well as apoptotic cells [4,27]. When imaging the effectiveness of chemotherapy, it maybe preferable to image cells that have died from either apoptotic or nonapoptotic mechanisms of cell death. Second, apoptotic cells are rapidly phagocytized in a process where PS recognition may play an important role [6,10,17,22]. This leads to the possibility that an NIRF signal may arise from phagocytic cells, which do not express extracellular-facing PS but have consumed NIRF apoptotic cells. Finally, PS exposure maybe reversible and precede a commitment to apoptosis [9].

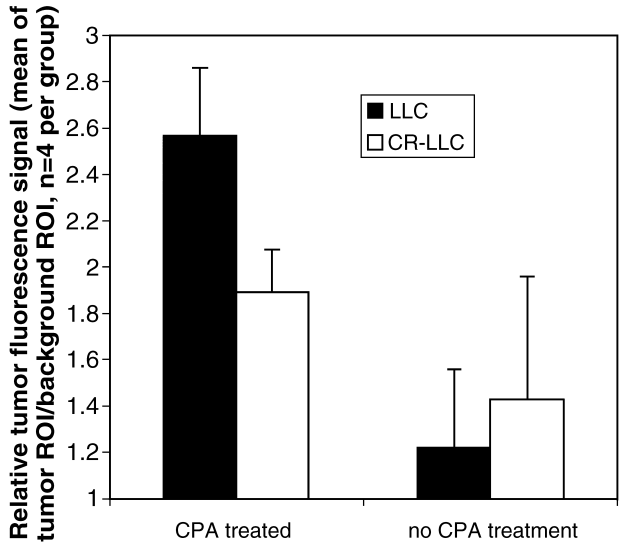

Figure 4. *TAR of animals injected with active Cy5.5–annexin V. Animals were CPA-treated or had no CPA treatment. Each animal contained CPA-sensitive LLC and CPA-resistant CR-LLC carcinoma, as shown in Figure 3. Values are means and standard deviations with four animals per group.*

The use of active Cy–annexin V and the simple reflectance NIRF imaging equipment we employed [13,28] provides a convenient method of imaging tumor PS exposure, which served as marker of tumor sensitivity to CPA treatment. Future studies based on this method will determine whether similar observations will apply with other tumor models. With humans, surface reflectance fluorescence imaging methods would seem to be impractical because of the longer distances light must traverse. However, the rapid development of fluorescence-mediated tomographic imaging methods now permits the quantitation of the NIRF signals emanating from sources deep within small animals [18–20] and may someday be used to image NIRF with humans. The acceptability of annexin V for use in human studies and the rapid development of NIRF-based imaging instrumentation may make the optical method for imaging of tumor PS, using an NIRF conjugate of annexin V, a clinical possibility.

Acknowledgements

We thank Allen Green and Theseus Imaging for the supply of annexin V.

References

[1] Blankenberg FG, Katsikis PD, Tait JF, Davis RE, Naumovski L, Ohtsuki S, Kopiwoda S, Abrams MJ, Darkes M, Robbins RC, et al. (1998). *In vivo* detection and imaging of phosphatidylserine expression during programmed cell death. *Proc Natl Acad Sci USA* **95,** 6349–54.

[2] Blankenberg FG, Naumovski L, Tait JF, Post AM, and Strauss HW (2001). Imaging cyclophosphamide-induced intramedullary apoptosis in rats using 99mTc-radiolabeled annexin V. *J Nucl Med* **42,** 309–16.

[3] Boehm T, Folkman J, Browder T, and O'Reilly MS (1997). Antiangiogenic therapy of experimental cancer does not induce acquired drug resistance. *Nature* **390,** 404–7.

[4] Dive C, Gregory CD, Phipps DJ, Evans DL, Milner AE, and Wyllie AH (1992). Analysis and discrimination of necrosis and apoptosis (programmed cell death) by multiparameter flow cytometry. *Biochim Biophys Acta* **1133,** 275–85.

[5] Ernst JD, Yang L, Rosales JL, and Broaddus VC (1998). Preparation and characterization of an endogenously fluorescent annexin for detection of apoptotic cells. *Anal Biochem* **260,** 18–23.

[6] Fadok VA, Bratton DL, Frasch SC, Warner ML, and Henson PM (1998). The role of phosphatidylserine in recognition of apoptotic cells by phagocytes. *Cell Death Differ* **5,** 551–62.

[7] Fisher DE (2001). Pathways of apoptosis and the modulation of cell death in cancer. *Hematol/Oncol Clin North Am* **15,** 931–56.

[8] Green AM, and Steinmetz, ND (2002). Monitoring apoptosis in real time. *Cancer J* **8,** 82–92.

[9] Hammill AK, Uhr JW, and Scheuermann RH (1999). Annexin V staining due to loss of membrane asymmetry can be reversible and precede commitment to apoptotic death. *Exp Cell Res* **251,** 16–21.

[10] Henson PM, Bratton DL, and Fadok VA (2001). Apoptotic cell removal. *Curr Biol* **11,** R795–805.

[11] Kohler G, Hering U, Zschornig O, and Arnold K (1997). Annexin V interaction with phosphatidylserine-containing vesicles at low and neutral pH. *Biochemistry* **36,** 8189–94.

[12] Lowe SW (1995). Cancer therapy and p53. *Curr Opin Oncol* **7,** 547–53.

[13] Mahmood U, Tung CH, Bogdanov Jr A, and Weissleder R (1999). Near-infrared optical imaging of protease activity for tumor detection. *Radiology* **213,** 866–70.

[14] Makin G, and Dive C (2001). Apoptosis and cancer chemotherapy. *Trends Cell Biol* **11,** S22–6.

[15] Martin SJ, Reutelingsperger CP, McGahon AJ, Rader JA, van Schie RC, LaFace DM, and Green DR (1995). Early redistribution of plasma membrane phosphatidylserine is a general feature of apoptosis regardless of the initiating stimulus: inhibition by overexpression of Bcl-2 and Abl. *J Exp Med* **182,** 1545–56.

[16] Mesner Jr PW, Budihardjo II, and Kaufmann SH (1997). Chemotherapy-induced apoptosis. *Adv Pharmacol* **41,** 461–99.

[17] Messmer UK, and Pfeilschifter, J (2000). New insights into the mechanism for clearance of apoptotic cells. *Bioessays* **22,** 878–81.

[18] Ntziachristos V, Bremer C, Graves EE, and Weissleder R (2002). *In vivo* tomographic imaging of near-infrared fluorescent probes. *Mol Imaging* **1,** 82–8.

[19] Ntziachristos V, Hielscher AH, Yodh AG, and Chance B (2001). Diffuse optical tomography of highly heterogeneous media. *IEEE Trans Med Imaging* **20,** 470–8.

[20] Ntziachristos V, Ripoli J, and Weissleder R (2002). Would near-infrared fluorescence signals propagate through large human organs for clinical studies? *Opt Lett* **27,** 333–5.

[21] Pigault C, Follenius-Wund A, Schmutz M, Freyssinet JM, and Brisson A (1994). Formation of two-dimensional arrays of annexin V on phosphatidylserine-containing liposomes. *J Mol Biol* **236,** 199–208.

[22] Platt N, da Silva RP, and Gordon S (1998). Recognizing death: the phagocytosis of apoptotic cells. *Trends Cell Biol* **8,** 365–72.

[23] Poot M, Gibson LL, and Singer VL (1997). Detection of apoptosis in live cells by MitoTracker red CMXRos and SYTO dye flow cytometry. *Cytometry* **27,** 358–64.

[24] Schmitt CA, and Lowe SW (2002). Apoptosis and chemoresistance in transgenic cancer models. *J Mol Med* **80,** 137–46.

[25] Span LF, Pennings AH, Vierwinden G, Boezeman JB, Raymakers RA, and de Witte T (2002). The dynamic process of apoptosis analyzed by flow cytometry using Annexin-V/propidium iodide and a modified *in situ* end labeling technique. *Cytometry* **47,** 24–31.

[26] van Engeland M, Nieland LJ, Ramaekers FC, Schutte B, and Reutelingsperger CP (1998). Annexin V affinity assay: a review on an apoptosis detection system based on phosphatidylserine exposure. *Cytometry* **31,** 1–9.

[27] Waring P, Lambert D, Sjaarda A, Hurne A, and Beaver J (1999). Increased cell surface exposure of phosphatidylserine on propidium iodide negative thymocytes undergoing death by necrosis. *Cell Death Differ* **6,** 624–37.

[28] Weissleder R, Tung CH, Mahmood U, and Bogdanov Jr A (1999). *In vivo* imaging of tumors with protease-activated near-infrared fluorescent probes. *Nat Biotechnol* **17,** 375–8.

[29] Ohtsuki K, Akashi K, Aoka Y, Blankenburg FG, Kpiwods S, Tait JF, and Strauss HW (1999). Techetium-99m HYNIC–annexin V: a potential radiopharmaceutical for the *in vivo* detection of apoptosis. *Eur J Nucl Med* **26,** 1251–8.

[30] Bhunchet E, Hatakawa H, Sakai Y, and Shibata T (2002). Fluorescein electronic endoscopy: a novel method for detection of early stage gastric cancer not evident to routine endoscopy. *Gastrointest Endosc* **55,** 562–71.

[31] Kobayashi M, Tajiri H, Seike E, Shitaya M, Tounou S, Mine M, and Oba K (2001). Detection of early gastric cancer by a real-time autofluorescence imaging system. *Cancer Lett* **165,** 155–9.